Carbohydrate Polymers 89 (2012) 1250–1260

Contents lists available at SciVerse ScienceDirect

Carbohydrate Polymers

journal homepage: www.elsevier.com/locate/carbpol

Properties of a novel type of starch found in the double mutant "sweet wheat"

Patricia L. Vrinten[a,c,1], Tomoya Shimbata[b,1], Michiyo Yanase[d], Ai Sunohara[b], Mika Saito[a], Takayuki Inokuma[b], Toshiyuki Takiya[b], Takeshi Takaha[d], Toshiki Nakamura[a,*]

[a] NARO Tohoku Agriculture Research Center, Morioka 020-0198, Japan
[b] Nippon Flour Mills Co., Ltd., Atsugi 243-0041, Japan
[c] Bioriginal Food and Science Corporation, Saskatoon, Canada S7J 0R1
[d] Ezaki Glico Co., Ltd., Osaka 555-8502, Japan

ARTICLE INFO

Article history:
Received 26 January 2012
Received in revised form 27 March 2012
Accepted 11 April 2012
Available online 1 May 2012

Keywords:
GBSSI
SSIIa
Sweet wheat
Wheat starch
Structural characteristics

ABSTRACT

The double mutant "sweet wheat" (SW), which produces substantial amounts of sugars in immature seeds, is missing two starch synthases, namely granule-bound starch synthase I (GBSSI) and starch synthase IIa (SSIIa). The lack of these two enzymes causes major changes in the attributes of SW seed, starch, and starch granules. SW seeds appear normal during early stages of development, but become shrunken when seeds begin to mature and dry. However, even in immature seed, starch granules are small and misshapen, and high levels of maltose are present throughout seed development. The crystallinity of SW starch is altered in that a major peak typical of the cereal A-type diffraction pattern is absent, and the gelatinization temperature of SW starch is considerably lower than that of wild-type starch. Amylopectin from SW seed has a substantially lower molecular weight than that from wild-type seed, and a low molecular weight peak with a bimodal distribution is found only in SW starch. This peak contains linear malto-oligosaccharides as well as short, branched glucans. SW starch has an increased proportion of branches with DP < 10, and chains with DP 2 and 3 are particularly increased. These changes suggest that sweet wheat starch is being modified in an atypical manner by isoamylases and/or β-amylases.
© 2012 Elsevier Ltd. All rights reserved.

1. Introduction

Starch is an important dietary source of calories for humans and domesticated animals, and also has many industrial uses (Ellis et al., 1998; Röper, 2002; Zeeman, Kossmann, & Smith, 2010), including serving as one of the major feedstocks for the production of biofuel (Balat & Balat, 2009; Demirbas, 2007; Naqvi et al., 2011; U.S. Department of Agriculture, 2011). Modifying the properties of starch produced by a plant can influence its suitability for different uses, and *in planta* modification of starch usually involves altering the enzymes involved in starch biosynthesis. The basic polymers of starch are amylose and amylopectin, which are produced from ADP-glucose by a set of enzymes which includes starch synthases, starch branching enzymes and starch debranching enzymes. Granule-bound starch synthase I (GBSSI) synthesizes the largely linear α-1,4 linked glucan amylose, and the absence of GBSSI results in an amylose-free or "waxy" phenotype. Synthesis of the branched amylopectin molecule is more complex, and in cereal endosperm starch involves the starch synthases SSI, SSIIa, and SSIII, a number of starch branching enzymes, and starch debranching enzymes (DBE) including isoamylase-type and pullulanase-type debranching enzymes. SSIIa in particular appears to have an important role in the synthesis of amylopectin in storage starch of cereals (Morell et al., 2003; Nakamura et al., 2005; Shimbata et al., 2005; Yamamori, Fujita, Hayakawa, Matsuki, & Yasui, 2000; Zhang et al., 2004). The absence of SSIIa generally results in a higher level of amylose, and in amylopectin with an increased number of short chain branches with a degree of polymerization (DP) of around 6–10, with a concurrent decrease in medium chain branches (DP 11–25).

In bread wheat, which is a hexaploid plant, the creation of starch synthesis mutants requires elimination of the gene products from the A, B and D genomes. The first line lacking all *GBSSI* gene products was developed by identifying lines with mutations in single genes, followed by crossing and selection to produce "waxy" wheat (Nakamura, Yamamori, Hirano, Hidaka, & Nagamine, 1995), and a similar approach was followed to produce wheat lines lacking all SSIIa proteins (Shimbata et al., 2005; Yamamori et al., 2000). By crossing the null GBSSI and SSIIa lines and using markers designed to distinguish null and wild-type alleles at all six loci (Nakamura, Vrinten, Saito, & Konda, 2002; Saito, Vrinten, Ishikawa, Graybosch, & Nakamura, 2009; Shimbata et al., 2005), we were able to select

* Corresponding author. Tel.: +81 196433514; fax: +81 196433514.
E-mail address: tnaka@affrc.go.jp (T. Nakamura).
[1] These authors contributed equally to this work and should be considered co-first authors.

0144-8617/$ – see front matter © 2012 Elsevier Ltd. All rights reserved.
http://dx.doi.org/10.1016/j.carbpol.2012.04.029

a GBSSI/SSIIa double null mutant (Nakamura et al., 2006). The double mutant, "sweet wheat" (SW) produced high levels of sugars, especially maltose, in immature seed. Mature SW seeds had a similar phenotype to mature seeds of sweet corn, with a shrivelled, shrunken appearance and a lower seed weight than wild-type wheat seeds. Here we elaborate on the changes in starch structure and starch granule morphology that occur in the double mutant.

2. Materials and methods

2.1. Selection of double mutant

The double mutant "sweet wheat" line was selected from the F3 progeny of a cross between a line carrying null alleles at all *GBSSI* loci and a line carrying null alleles at all *SSIIa* loci using PCR-based markers (Nakamura et al., 2006). To confirm the absence of GBSSI and SSIIa proteins, one-dimensional SDS-PAGE analysis of starch granule proteins was conducted as previously described (Nakamura, Yamamori, Hirano, & Hidaka, 1993), and proteins were visualized using a silver staining kit (Wako Chemicals, Osaka, Japan).

2.2. Plant material

Materials used in this study included the double mutant SW line described above, the *waxy* (Wx) wheat breeding line K-2, the high amylose (HA) mutant line developed in our previous work (Shimbata et al., 2005), and the wild-type control cultivar Chinese Spring. Plants were grown in a temperature-controlled greenhouse (22 °C day/15 °C night).

2.3. Starch extraction

Starch was extracted from flour using SDS buffer according to the method of Echt and Schwartz (1981) with minor modifications. Rather than using a homogenizer, flour in SDS buffer (1% SDS (w/v), 0.5 M Tris–HCl pH 6.8) was shaken in 1.5 mL eppendorf tubes on a rotary shaker at 200 rpm for one hour to avoid breakage of starch granules. The mixture was then centrifuged at 17,000 × *g* to precipitate granules. The upper phase was removed without interfering with the surface of the starch granules. Next, starch granules were washed with excess milliQ water on a rotary shaker for 5 min, centrifuged, and excess water was removed. This water wash was performed five times. Acetone was then added and starch granules were air-dried at room temperature while slowly turning the tube to avoid aggregation of starch granules.

2.4. Microscopic analysis

To investigate starch granule morphology during development, granules from mature seed and immature endosperm tissue (25 DPA) were stained with iodine and potassium iodide solution (0.2% KI, 0.04% I_2) and observed under an optical microscope (Olympus, Tokyo, Japan). Scanning electron microscopic analysis was conducted with a VE-8800 Keyence (Osaka, Japan) microscope. Starch granules were directly scanned at 1.3 kV without gold coating.

2.5. Amylose quantification and maximum absorbance

Amylose content was determined with an AutoAnalyzer (Bran + Luebbe, Tokyo, Japan) using the method of Kuroda, Oda, Miyagawa, and Seko (1989) as described by Nakamura, Vrinten, Hayakawa, and Ikeda (1998). The maximum absorbance (λ_{max}) of the iodine–starch complex was determined according to Konishi, Nojima, Okuno, Asaoka, and Fuwa (1985).

2.6. High-performance size-exclusion chromatography (HPSEC)

Starch granules were defatted according to Hayakawa, Tanaka, Nakamura, Endo, and Hoshino (1997), after which 2 mg of starch granules were dispersed overnight in 100 μL of dimethylsulfoxide (DMSO) at room temperature. Isoamylase debranching was performed according to Hayakawa et al. (1997). Samples treated with heat-inactivated isoamylase were used as controls. HPSEC was performed on a LaChrom Elite HPLC system including an HPLC-pump (L-2130), refractive index detector (L-2490) (Hitachi High-Technologies, Tokyo, Japan) and column oven (865-CO, Jasco, Tokyo, Japan) controlled by EZ Chrom Elite version 3.1.5aj software. The column oven and detector temperatures were set at 60 °C and 45 °C, respectively. Separation was performed on OHpak SB-G guard (Shodex, Tokyo, Japan) and OHpak SB-804 HQ separation (φ 8.0 mm × 300 mm) (Shodex, Tokyo, Japan) columns, with 10 mM sodium acetate buffer (pH 6.0) containing 0.1 M NaCl as eluent at a flow rate of 0.5 mL/min. Maltoheptaose (Nacalai Tesque, Kyoto, Japan) and pullulan standards (Shodex, Tokyo, Japan) were used as molecular weight standards. The SW fraction containing the low molecular weight bimodal peak (retention time 17.0–20.5 min) was collected and dried with a vacuum concentrator. After dispersing in DMSO, the sample was treated with isoamylase or heat-inactivated isoamylase, then again subjected to HPSEC analysis. The chain length distribution was determined by the FACE method as described below.

2.7. Fluorophore-assisted carbohydrate electrophoresis (FACE)

The FACE technique of Morell, Samuel, and O'Shea (1998) was followed, with some modifications. After isoamylase treatment, samples were dried with a vacuum concentrator. Fluorescent labelling of reducing residues was conducted using an eCAP™ N-linked oligosaccharide profiling kit (Beckman Coulter, CA) and separation of oligosaccharides was performed with the P/ACE system 5000 with a P/ACE system Laser Module 488 controlled by P/ACE station software (Beckman Coulter, CA).

2.8. Gel filtration chromotography

Gel filtration was performed with a Sephacryl S-1000 SF column (GE Healthcare Japan, Hino, Japan) at a flow rate of 1 mL/min using 150 mM NaOAc (pH 5.5) as an eluent. Samples were applied in a total volume of 3 mL (0.4% (w/v) starch, 30% (v/v) DMSO, 150 mM NaOAc (pH 5.5)). Total carbohydrates were measured using the phenol–sulfuric acid colorimetric method. Amylose percent was calculated as described by Hovenkamp-Hermelink et al. (1988). Amylopectin was calculated as total carbohydrates minus amylose. The amylopectin fractions obtained by filtration were precipitated by ethanol and dissolved in DMSO to give a final concentration of 1% (w/v) and used for chain length distribution analysis by HPAEC-PAD.

2.9. High-performance anion exchange chromatography with pulsed amperometric detection (HPAEC-PAD)

HPAEC-PAD was carried out with a Dionex DX-300 system using a CarboPack PA-100 (Nihon Dionex, Osaka, Japan) column. Samples were applied in 25 μL, with a final starch concentration of 0.2% (w/v). Samples were eluted with a gradient of NaOAc (50–850 mM) in 150 mM NaOH at a flow rate of 1 mL/min.

2.10. Ethanol fractionation of SW starch

SW starch granules prepared as described above were dissolved in DMSO to a concentration of 0.5% (w/v). Ethanol was added to

achieve a 1:1 ratio of starch solution:ethanol, and the solution was centrifuged. The precipitate was analysed by HPSEC and the chain length distribution profile was obtained as described above, while glucans remaining in the supernatant were precipitated using an increased ratio of ethanol: starch solution. This step was repeated several times, giving 5 fractions, the final of which was precipitated with 9 parts ethanol: 1 part starch solution.

The fraction obtained from the final precipitation was further analysed by digestion with additional amylases. Reactions were performed in a total volume of 50 μL including 10 μL 0.5% SW starch, 25 μL 20 mM NaOAc (pH 5.5), plus either 5 μL glucoamylase (500 U/mL), 5 μL β-amylase (200 U/mL), 5 μL isoamylase (500 U/mL) or 5 μL each isoamylase and β-amylase. After incubation at 37 °C for 2 h, the enzymes were heat-denatured at 100 °C for 10 min, the solution was centrifuged, and the supernatant was subjected to HPAEC-PAD analysis as described above.

2.11. Measurement of maltotriose levels

Maltotriose levels were measured as described previously (Nakamura et al., 2006).

2.12. Differential scanning calorimetry (DSC)

Starch gelatinization properties were analysed using a differential scanning calorimeter (DSC-60A, Shimadzu, Kyoto, Japan) according to Fujita, Yamamoto, Sugimoto, Morita, and Yamamori (1998). For SW, the total precipitated starch granule sample was analysed.

2.13. X-ray diffraction

X-ray diffraction measurements were conducted according to Hayakawa et al. (1997) using a diffractometer X'pert PRO MPD (Panalytical, Netherlands) operated at 40 mA and 50 kV. The diffraction angle (2θ) was scanned from 4° to 30° with a 0.004° step size.

3. Results

3.1. SW lacks all GBSSI and SSIIa proteins

The SW double mutant used in this work was selected by screening with allele-specific PCR-based markers as previously described (Nakamura et al., 2006). One dimensional SDS-PAGE analysis was used to confirm the results of PCR-based screening, and clearly demonstrated the absence of all GBSSI and SSIIa proteins in SW (Fig. 1). The reduction in intensity of the two bands directly below the SSIIa bands, which correspond to starch granule protein (SGP)-2 or SBEII, and SGP-3 or SSI, was also noted in the HA wheat mutant by Yamamori et al. (2000). The reduction in SGP-2 and SGP-3 intensity is maintained in SW (Fig. 1).

3.2. Starch granules of SW have a novel morphology

Starch granules from SW reacted differently to washing and precipitation than granules from other genotypes. Granules from wild-type (Fig. 2A) and SW parental lines (not shown) formed a firm pellet after centrifugation, but only a small portion of SW granules formed such a pellet. Instead, most of the SW precipitate consisted of a gelatinous mass (Fig. 2A). When starch granules were spread out and allowed to air-dry, the dry film formed by SW starch granules, particularly granules from the upper portion, became shrunken and cracked. The gel-like upper phase was also present when starch granules were extracted using water alone (results not shown). Films, fillers and composites made from or including starches have many food and non-food uses (Xie, 2011; Yu, Dean, & Li, 2006), and clearly SW starch has novel properties for such applications.

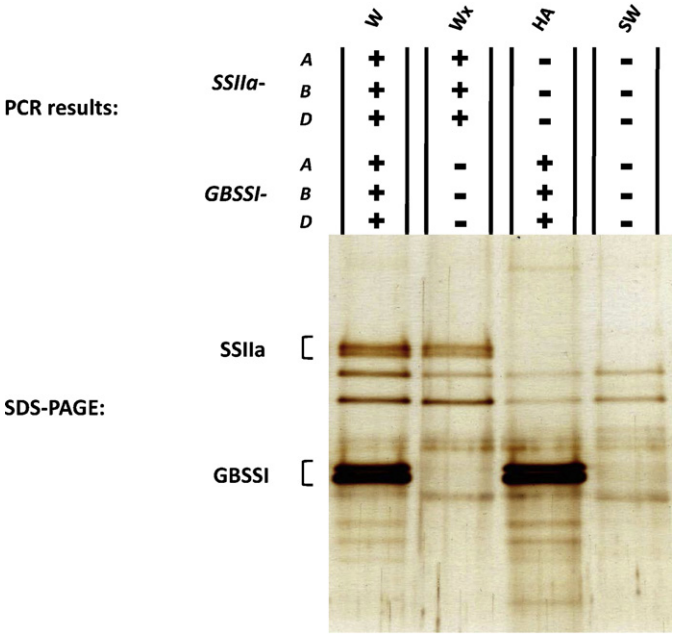

Fig. 1. SW lacks GBSSI and SSIIa proteins. PCR-based marker-assisted selection results (top panel) were confirmed by SDS-PAGE (bottom panel). The Wx parent lacks all GBSSI proteins (lane 2), the HA parent lacks all SSIIa proteins (lane 3), and the SW line lacks both sets of proteins (lane 4). The double band for the SSIIa proteins results from separation of SSIIa-B1 (bottom band) from SSIIa-D1 and -A1 proteins, while the double band for the GBSSI proteins results from separation of Wx-A1 protein (top band) from Wx-B1 and -D1 proteins. W, wild-type; Wx, waxy; HA, high amylose; and SW, sweet wheat.

Although we could not distinguish starch granules in the dried upper portion of the SW precipitate with a light microscope, electron microscopic analysis showed this mass consisted of very small, tightly bound granules (Fig. 2B), the majority of which were considerably smaller than the small "B-type" granules found in wild-type wheat. Even those SW starch granules that did precipitate into a pellet were not normally shaped, but were small and malformed, and appeared deflated compared to the pancake-like granules of wild-type wheat (Fig. 2B). Starch granules from the HA line had a somewhat deflated appearance and often showed the presence of fissures, as has been previously reported (Yamamori et al., 2000). As expected, the starch of the SW double mutant was amylose-free and stained red-brown with iodine (Fig. 2B). The lack of amylose in this genotype was confirmed by a colorimetric analysis (Fig. 2C). This analysis also indicated that SW had a lower maximum absorbance value (λ_{max}) than did waxy wheat.

3.3. Abnormalities in SW starch granules are detectable earlier than seed shape abnormalities, and are accompanied by increased maltotriose levels

Previously, we determined that mature SW seed has a shrivelled phenotype, which is accompanied by a reduction in kernel weight of approximately 30% (Nakamura et al., 2006). Here, we investigated changes that occur in seed shape throughout seed development. SW seeds appeared normal at early developmental stages, but began to lose volume by 35 days post-anthesis (DPA), and had a collapsed appearance by physiological maturity at 45 DPA (Fig. 3A).

The normal, plump appearance of SW seed at 25 DPA led us to question whether SW starch granules also had a normal shape at early stages of seed development, and underwent

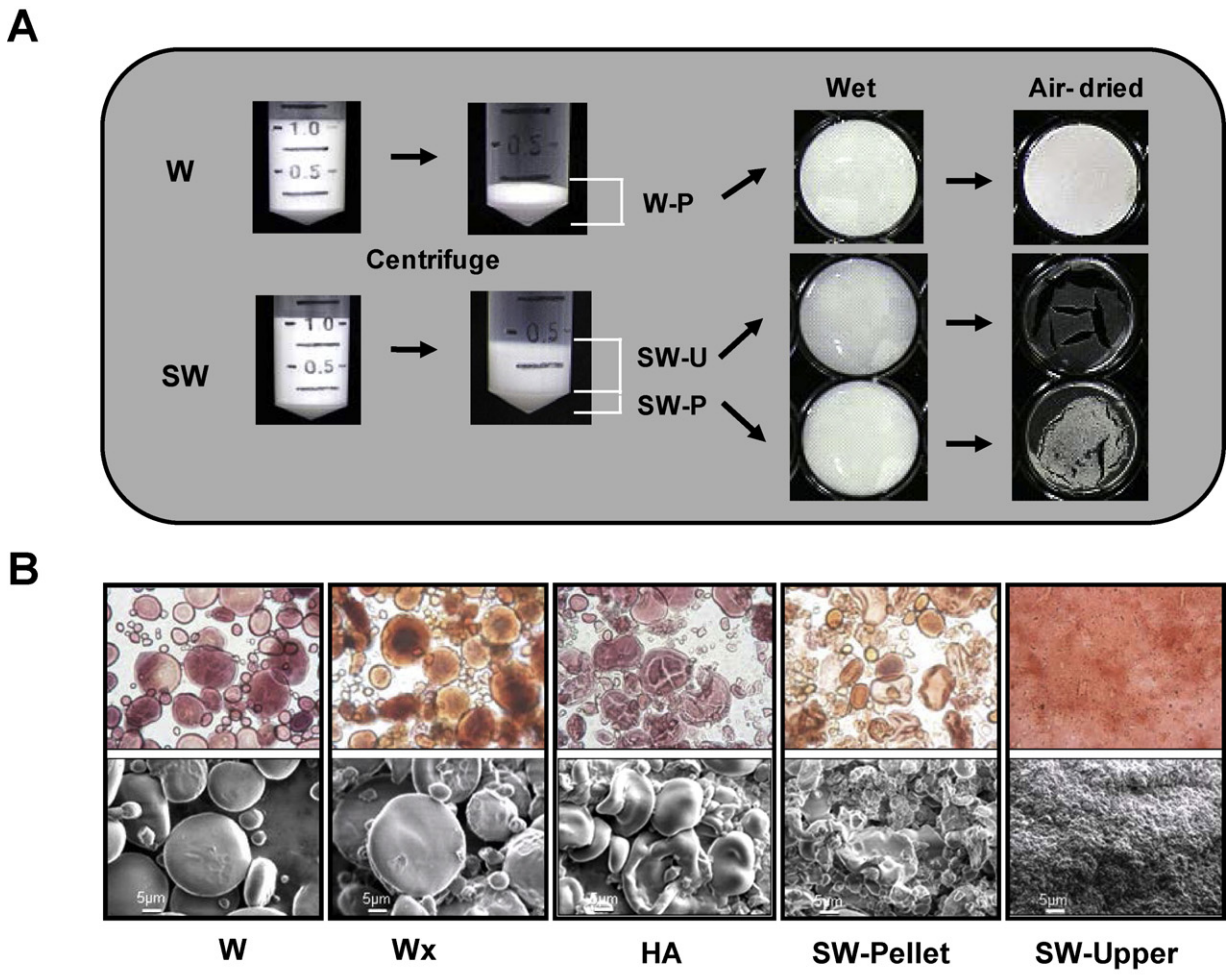

Fig. 2. Starch granule morphology and amylose content of starch. (A) Effect of genotype on precipitation of starch granules from mature seeds. 100 mg of starch was suspended in 1 mL water and centrifuged at 17,000 × *g* for 10 min, causing starch granules (SGs) of wild type (W) to precipitate, forming a pellet. SGs of SW also precipitated but only the bottom portion of the precipitate formed a pellet (SW-P), while the upper portion of the SW sediment (SW-U) formed a clear gel on top of the pellet. (B) Isolated SGs from mature seed as observed under a light microscope after iodine staining (upper panels) and as observed under an electron microscope (lower panels). (C) Wave length indicating maximum absorbance (λ_{max}) of dissolved starch treated with an iodine solution. Amylose content was determined by a colorimetric iodine-binding assay using 100 mg of SGs per dish.

degradation during seed maturation. However, as shown in Fig. 3B, SW starch granules in fresh endosperm tissue collected at 25 DPA possessed the same small, misshapen appearance as starch granules obtained from mature seed. Other genotypes also maintained a typical, genotype-specific starch granule shape between 25 DPA and seed maturity (Figs. 2B and 3B).

High levels of maltose were previously detected in SW seed throughout seed development, with particularly high levels present in immature seed (Nakamura et al., 2006; Shimbata et al., 2011). At 25 DPA, maltose levels average over 30 μg/mg fresh weight in SW seed, but is barely detectable in wild-type seed (Nakamura et al., 2006). Here, we determined that maltotriose levels in SW followed a similar pattern, peaking at 25 DPA, prior to seed shrivelling, but remaining considerably higher in SW than in other genotypes throughout seed development (Fig. 4). Maltose is normally produced from starch by β-amylase, and maltotriose can also be a product of this enzyme.

3.4. SW starch has a low peak gelatinization temperature

The peak gelatinization temperature (T_p) of waxy wheat was slightly higher than that of wild-type (Table 1), in agreement with other studies suggesting that a lack of amylose leads to an increase in gelatinization temperature (Mangalika, Miura, Yamauchi, & Noda, 2003; Tester & Morrison, 1990). The DSC peak of SW was somewhat broad, which may reflect the novel amylopectin chain

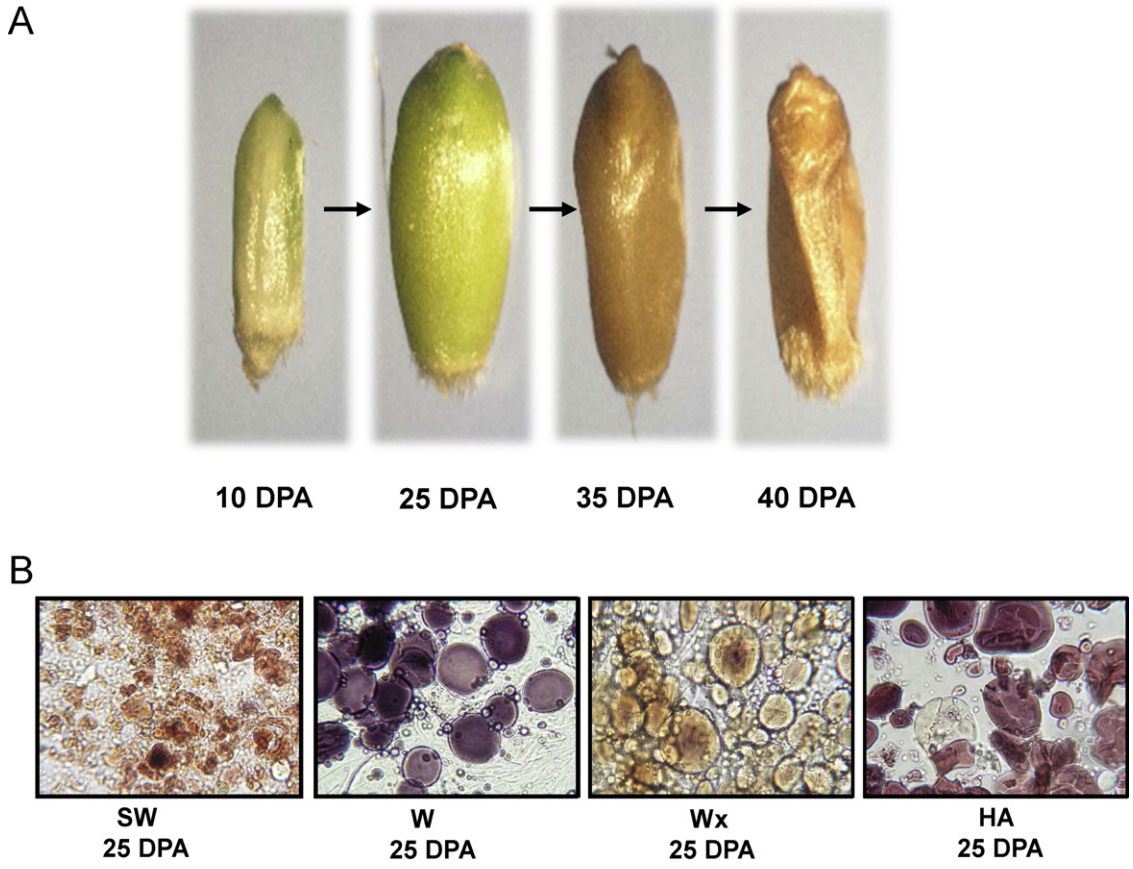

Fig. 3. Appearance of SW seed during seed development and shape of starch granules from immature seeds. (A) Changes in SW seed shape occurring from 10 to 40 days post-anthesis (DPA). (B) Shape of starch granules in immature endosperm tissue collected at 25 DPA. Sliced cross-sections of endosperm were stained with iodine and observed with a light microscope. W, wild-type; Wx, waxy; HA, high amylose; and SW, sweet wheat.

length distribution in this line. However, the peak gelatinization temperature of SW was very similar to the low peak temperature of the HA parent (Table 1). Thus, the characteristics of amylopectin chains conditioned by SSIIa had a much larger effect on gelatinization than the presence or absence of amylose. A large scale study of rice genotypes suggested that DSC methodology achieves the most specific values for gelatinization temperature (Cuevas et al., 2010) and also determined that SSIIa genotype had the largest effect on gelatinization temperature, in concurrence with the results obtained here (Table 1). As expected, a second amylose–lipid dissociation peak was only detected in the amylose-producing lines (W and HA, Table 1).

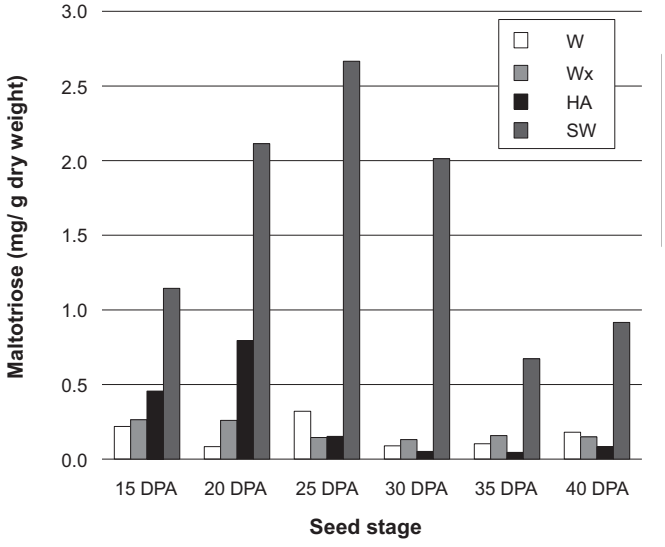

Fig. 4. Accumulation of maltotriose during seed development. The level of maltotriose in SW seeds peaks at 25 DPA, but remains higher than levels in other genotypes throughout seed development. W, wild-type; Wx, waxy; HA, high amylose; and SW, sweet wheat.

3.5. SW starch has novel structural characteristics

HPSEC analysis was used to compare the structure of SW starch to that of wild-type and parental lines (Fig. 5). Clear peaks

Table 1
DSC analysis of starch gelatinization.

	Gelatinization Peak				Amylose-Lipid Dissociation Peak			
	To[a] (°C)	*Tp*[b] (°C)	*Tc*[c] (°C)	*ΔH*[d] (J/g)	*To* (°C)	*Tp* (°C)	*Tc* (°C)	*ΔH* (J/g)
W	55.5	60.2	65.9	10.1	91.0	95.4	100.2	1.2
Wx	57.2	63.1	73.5	13.6	ND	ND	ND	ND
HA	44.8	50.2	55.1	5.0	87.9	93.5	98.6	2.1
SW	43.4	48.5	61.9	5.9	ND	ND	ND	ND

[a]Onset temperature.
[b]Peak temperature.
[c]Completion temperature.
[d]Enthalpy.

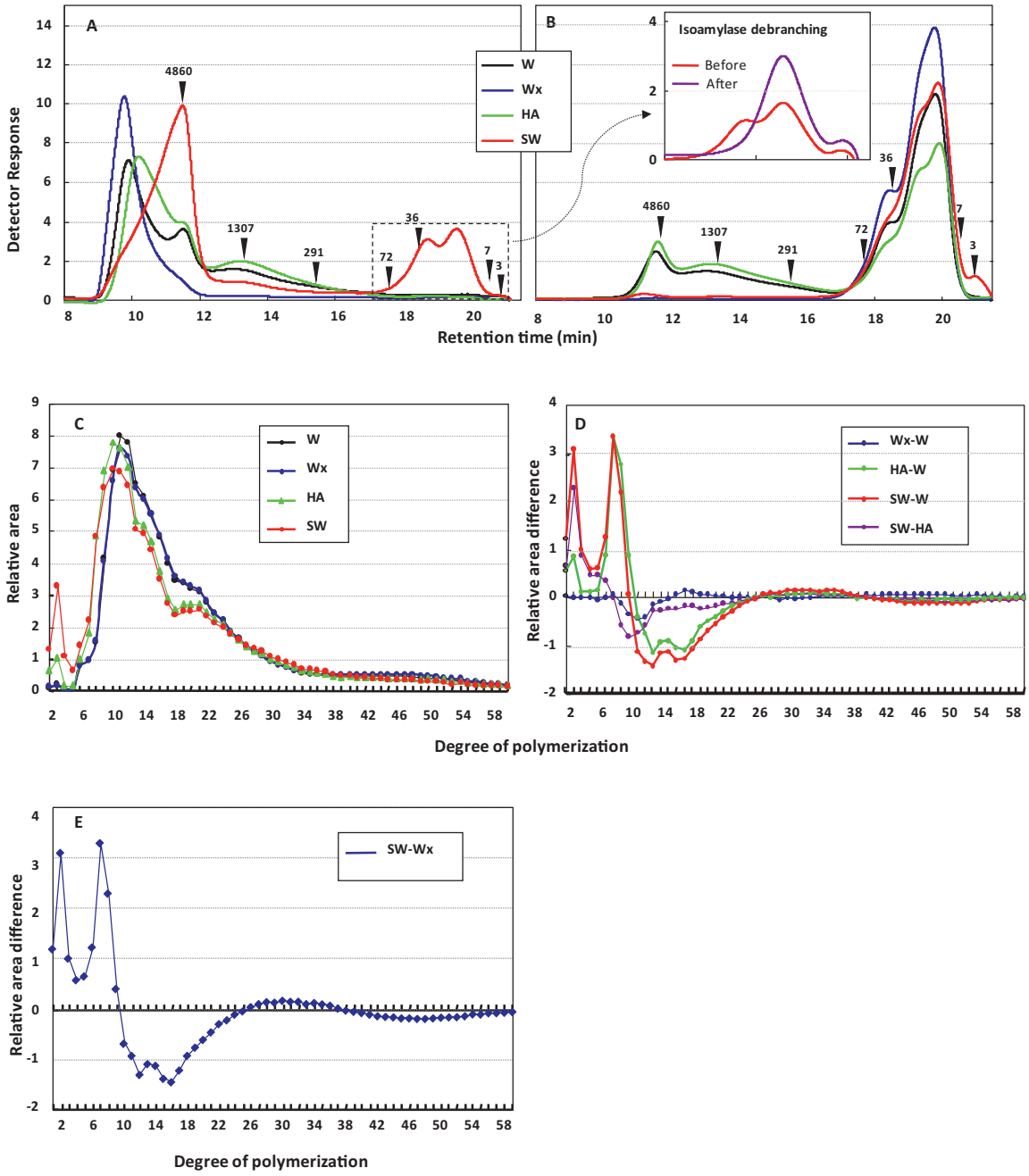

Fig. 5. Polymerization profiles of α-glucans. (A) Size fractionation of glucan polymers from undigested starches as obtained by high performance size-exclusion chromatograpy (HPSEC). (B) Size fractionation of glucan polymers from isoamylase-debranched starch. Arrowheads indicate chain lengths of malto-oligosaccharides (DP = 3 and 7) and pullulan-based standards. Inset: fractions representing a unique peak observed only in SW (dotted box in (A)) were collected and re-fractionated before and after isoamylase debranching. The chain length (DP14) for the highest point of the debranched peak was obtained using fluorophore-assisted carbohydrate electrophoresis (FACE). (C) Chain length distributions of isoamylase-debranched starches, as determined by the FACE method. (D) Differences in chain length distributions, obtained by subtracting the relative area of W from Wx, W from HA, W from SW, and HA from SW. (E) Differences in chain length distributions between SW and Wx.

representing amylose and amylopectin are present in starch from wild-type wheat, whereas the amylose peak is missing in Wx and SW starch (Fig. 5A). Amylopectin from SW starch has a much lower molecular weight than amylopectin from wild-type wheat, such that the SW amylopectin peak overlaps with the wild-type amylose peak. A second, broad amylopectin peak is present in SW but not in Wx at an elution time of about 12–15 min; this peak also overlaps with lower molecular weight amylose species from HA and W starch. Interestingly, a novel bimodal peak was identified only in SW. This bimodal peak represents glucans of low molecular weight, with a DP of less than 75 (Fig. 5A, dotted box).

After isoamylase debranching (Fig. 5B), the amylopectin peaks in Wx and SW completely disappear and are replaced by peaks of lower molecular weight, overlapping with the SW bimodal peak. When glucans from the unique SW bimodal peak were subjected to debranching (Fig. 5B, inset), the first peak disappeared, while the height of the second peak increased. Thus, the first glucan peak represents branched molecules, while the second peak, which was unaffected by the debranching treatment, appears to contain linear malto-oligosaccharides (MOS). The most common chain length (DP14) of the debranched SW-specific peak was obtained by using

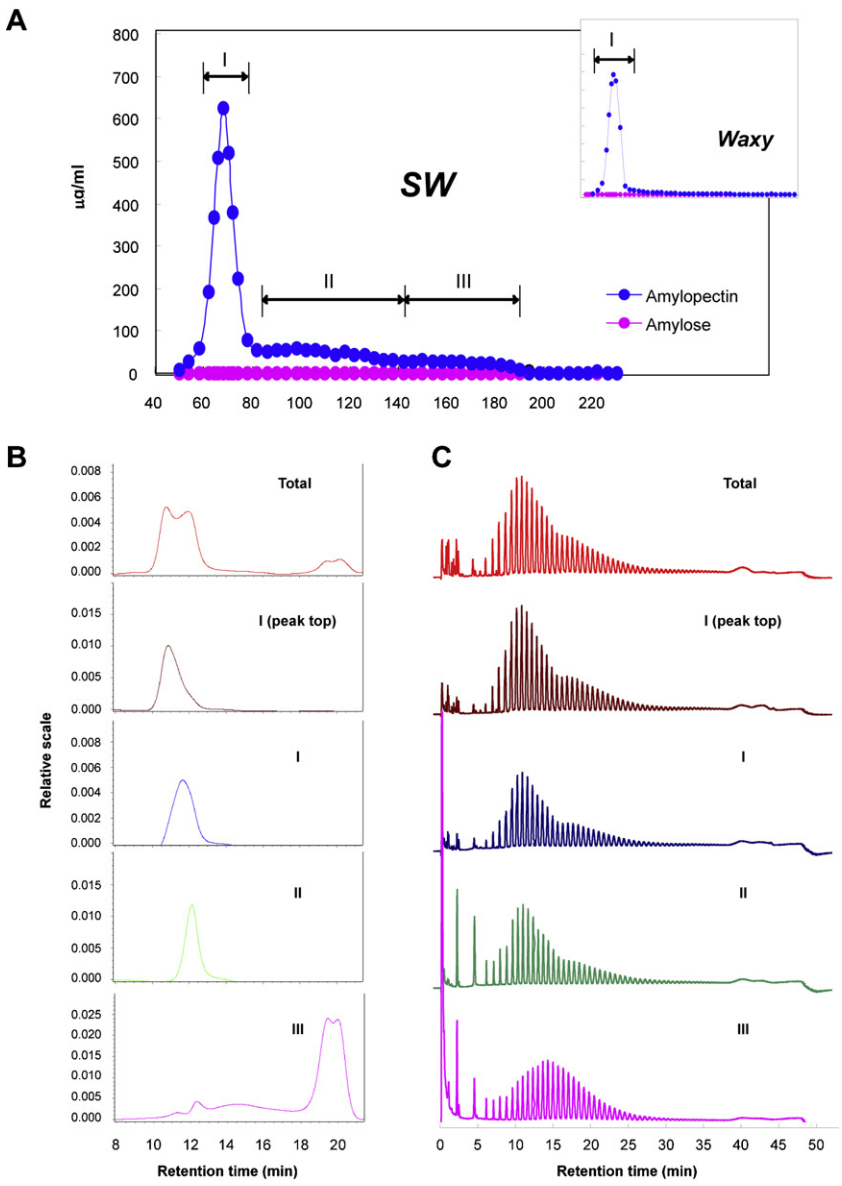

Fig. 6. SW amylopectin structure is non-uniform. (A) Starch was separated by gel filtration chromatography. Three amylopectin peaks were detected in SW (I–III), while a single amylopectin peak was detected in all other genotypes, as illustrated by the chromatograph from the Waxy genotype (inset). (B) Collected SW fractions were analysed by HPSEC before debranching with isoamylase. (C) After isoamylase digestion, samples were analysed by HPAEC-PAD. The chain-length distribution profile of fractions varied, and the highest proportion of short chains was detected in the low-molecular-weight fraction (III).

fluorophore-assisted carbohydrate electrophoresis (FACE) (see Supplementary data).

To investigate differences in chain length profiles, debranched starches from all genotypes were separated according to degree of polymerization (DP) using the FACE method (Fig. 5C–E). In both SW and HA, the relative number of short (DP < 10) chains increased, while medium-sized chains (DP11–25) decreased. There also appeared to be a slight increase in the level of long (DP > 25) chains. Similar trends have been observed in SSII mutants of other plants (Craig et al., 1998; Morell et al., 2003; Zhang et al., 2004). However, in SW the relative amount of very short chains (DP2–5), particularly the amount of DP3 chains, increased to a much higher level than was seen in the SSIIa mutant HA line, as is clearly indicated by the graph representing the difference between the relative areas of SW and HA (Fig. 5D). The graph showing the differences between SW and Wx (Fig. 5E), neither of which contain amylose, is very similar to the graph representing the SW-wild-type differential (Fig. 5D).

To verify and expand on the results described above, a large-scale separation of SW starch using gel-filtration chromatography (Fig. 6A) was used to provide information on the chain-length distribution within various fractions of SW starch. As expected, a single major amylopectin peak was detected by gel-filtration in starch samples from wild-type and parental genotypes, as is demonstrated with the sample from Wx wheat (Fig. 6A). However, three amylopectin peaks were detected in SW (Fig. 6A; I–III). To compare the structure of amylopectin within these peaks, fractions were collected and analysed by HPSEC (Fig. 6B). The bimodal peak was identified in the last of these fractions, confirming the results shown in Fig. 5A. Interestingly, the first, highest molecular weight fraction of undigested SW starch also had a bimodal distribution (Fig. 6B, top panel), which resulted in two distinct peaks when this region was separated into two fractions (Fig. 6B, second and third panels). HPAEC-PAD analysis of individually collected fractions treated with isoamylase indicated that the low molecular weight fraction containing the bimodal peak had the highest

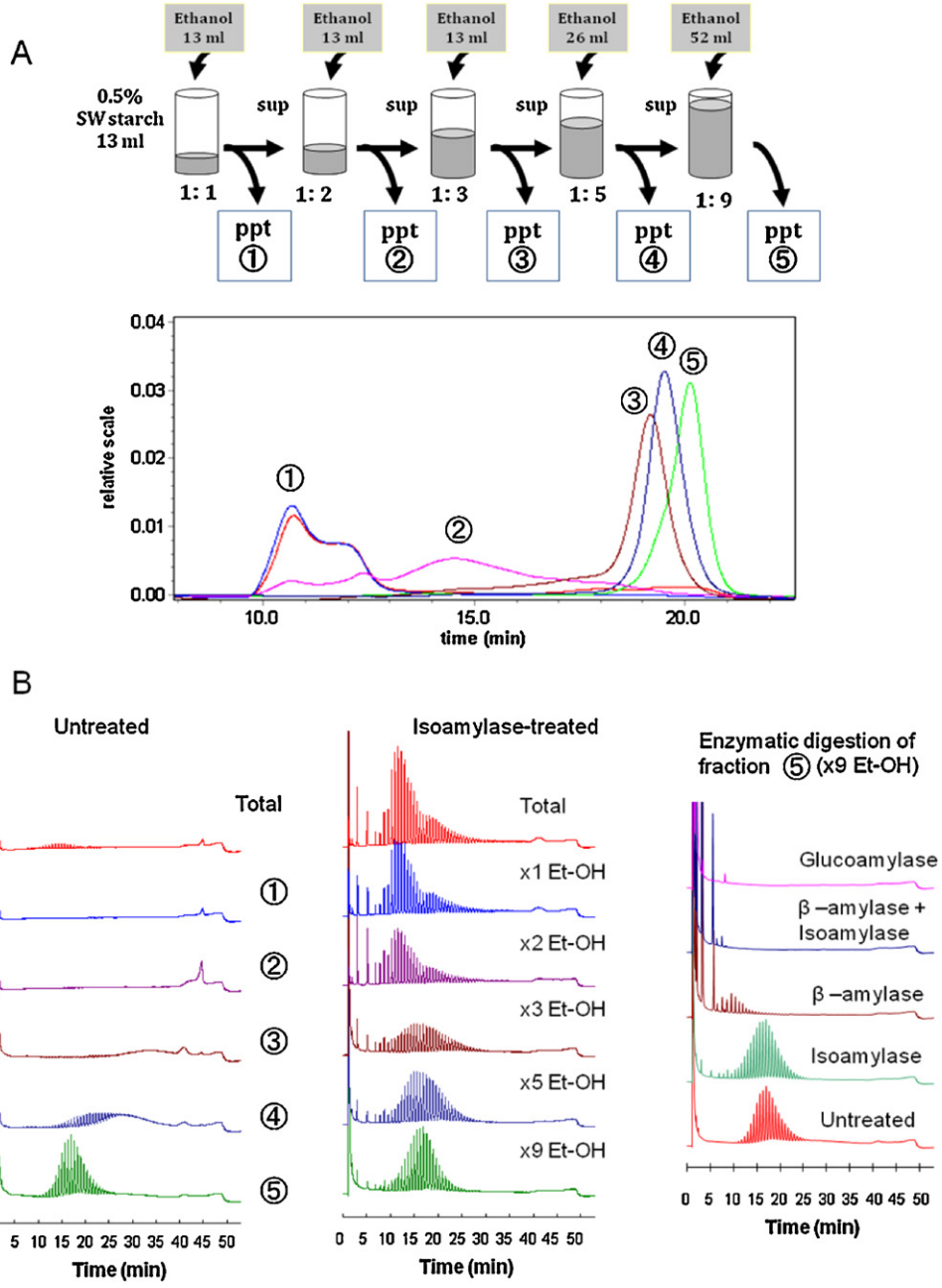

Fig. 7. SW starch granules contain low-molecular-weight linear molecules. (A) Isolated starch granules dissolved in DMSO were precipitated with varying concentrations of ethanol and separated by HPSEC. Lower sized glucans were precipitated by increasing concentrations of ethanol. (B) Collected SW starch fractions were analysed by HPAEC-PAD, either before (left panel) or after (centre panel) debranching with isoamylase. The chain length profile of the glucans precipitated with 9× EtOH did not change after isoamylase digestion (right panel), indicating this fraction represented mostly linear malto-oligosaccharides. However the slight change in profile after digestion with β-amylase plus isoamylase, as compared to β-amylase alone (right panel), indicated the presence of some branches in this fraction.

proportion of short chains (Fig. 6C). The presence of additional amylopectin peaks in SW, in combination with the variability in chain length distributions between these peaks, indicates that SW amylopectin has a less homogeneous structure than wild-type or waxy wheat amylopectin.

We further investigated the composition of SW starch by subjecting a solubilized starch solution to stepwise precipitations with increasing proportions of ethanol (Fig. 7). The glucans remaining after each precipitation tended to be smaller in size, and the final precipitate that was recovered using a 1:9 ratio of starch solution to ethanol contained mostly linear MOS. In this fraction, the profile prior to digestion with isoamylase resembled the isoamylase-digested chain length distribution (Fig. 7B, bottom panels) although comparison of the profile after digestion with β-amylase versus β-amylase plus isoamylase indicated some branched structures were present.

3.6. X-ray diffraction pattern of SW starch differs from normal cereal pattern

The X-ray diffraction (XRD) pattern of SW shows substantial changes from the wild-type pattern (Fig. 8). The peak at 18°, which is characteristic of the A-type starches of cereals and is clearly visible in CS, is not present in SW. As well, the peak at 22° is flattened out substantially in SW, and a minor peak is visible at 5°. The HA line was dominated by a flat peak at 20°, while the pattern from

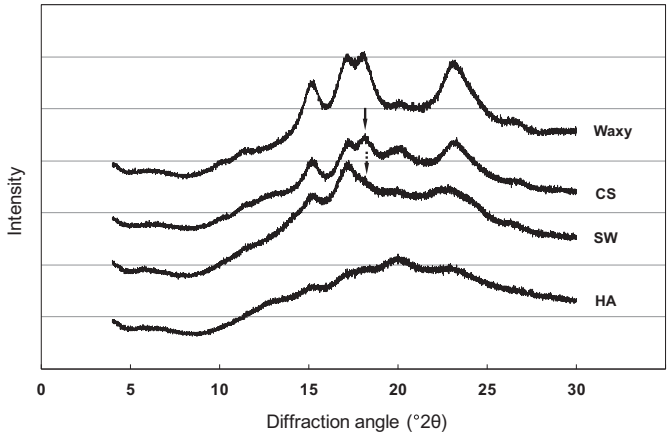

Fig. 8. X-ray diffraction patterns for starches from various genotypes. Patterns were obtained with Cu Kα radiation. The peak at 18° (arrow), which is normally found in the A-type starches of cereals but not in B-type starches of potato or C-type starches of pea, is absent from the SW sample. Waxy, waxy; HA, high amylose; CS, Chinese Spring; and SW, sweet wheat.

waxy starch closely resembled that of wild-type (CS), except for the absence of a minor peak at 20°.

Typically, in the A-type starches found in cereals, XRD patterns show major peaks at 2θ values of 15°, 17°, 18°, 20° and 23°. Conversely, in the B-type starches found in tubers, a major peak is present at around 5°, the peak at 15° is much flatter, and peaks at 18° and 23° are absent, while additional peaks are present at 22° and 24° (Cheetham & Tao, 1998). The SW diffractogram (Fig. 8) shows some of the characteristics of this B-type pattern, although the peak at 23° has flattened out considerably and has not resolved into a doublet, and the peak at 5° is not as distinct as is normally found in B-type starches. The pattern in SW may more closely resemble a C-type pattern (Cheetham & Tao, 1998), which is characteristic of legume starch, and is thought to be a mixture of A- and B-polymorphs (Gernat, Radosta, Damaschun, & Schierbaum, 1990). The XRD pattern for the SSIIa mutant line resembled a low crystallinity B-type pattern dominated by a flat peak at a 2θ value of 20° (Fig. 8). Konik-Rose et al. (2007) also obtained an XRD pattern for the SSIIa mutant dominated by a peak at 20°. This peak is characteristic of V-type polymorphs (Shi, Capitani, Trzasko, & Jeffcoat, 1998; Cheetham & Tao, 1998; Singh, Cairns, Morris, & Smith, 1998), which represent single-helical amylose molecules complexed with molecules such as lipids (Buléon, Véronèse, & Putaux, 2007). In SW, the relatively clear XRD pattern observed (Fig. 8) may be partially due to the lack of amylose, and consequently the lack of V-type polymorphs. In general, lower amylose levels have been associated with higher levels of crystallinity (Cheetham & Tao, 1998; He, Song, Ruan, & Chen, 2006; Vandeputte, Derycke, Geeroms, & Delcour, 2003; Yoo & Jane, 2002).

4. Discussion

Initially, we expected that lines without GBSSI or SSIIa activity would produce starch lacking amylose, but otherwise resembling starch from the SSIIa mutant. In fact, the double mutant has many unique characteristics not found in either of the parental lines. While SW seed shape resembles that of wild-type and parental lines during the early developmental stages, seed shrivelling is apparent by 35 DPA (Fig. 3A). This change in seed morphology was reflected in a change in starch granule morphology, with the granules from SW having a distinctive, shrunken appearance (Figs. 2A and 3). Particularly, a population of small, misshapen starch granules was found only in SW (Fig. 2B), and these abnormalities in starch granule development were apparent at early stages of starch granule development (Fig. 3B), well before changes in seed shape were noted. The small size of starch granules in SW may result from inefficient granule growth due to the absence of two major starch synthesis enzymes, GBSSI and SSIIa. However, the lower molecular weight of amylopectin in SW, in combination with the high number of DP2 and DP3 branch chains and the presence of maltose and maltotriose, suggested that starch synthesis and hydrolysis were occurring simultaneously in SW.

Some of the changes detected in SW starch are identical to effects that would be expected from β-amylase activity on starch. For example, digestion of waxy maize starch granules with β-amylase resulted in an increase in the proportion of chains with 2–5 glucose units, as well as an increase in soluble sugars (Mendez-Montealvo, Wang, & Campbell, 2011). Similar features are detected in SW, which shows an increased level of maltose in both immature and mature seed (Nakamura et al., 2006; Shimbata et al., 2011), and also shows a dramatic increase in glucans with a DP of 2–5 (Fig. 5). The presence of maltose and maltotriose early in SW seed development implies that β-amylase comes into contact with SW starch granules prior to seed desiccation. This would necessitate either localization of β-amylase to amyloplasts, which to our knowledge has not been demonstrated to date, or modification of membrane integrity in SW amyloplasts, resulting in exposure of starch granules to β-amylase produced and stored outside the amyloplast. An example of this type of plastid disruption is seen in *Arabidopsis* leaves, where the accumulation of malto-oligosaccharides in mutant phenotypes is associated with chloroplast degradation (Stettler et al., 2009).

However, regardless of how hydrolytic enzymes come into contact with SW starch granules, raw starch is normally considered to be resistant to hydrolysis by β-amylase (Sarikaya, Higasa, Adachi, & Mikami, 2000), suggesting that changes in the structure of SW starch are important in making it more susceptible to hydrolysis. Blazek and Copeland (2010) demonstrated that plant genotype can have a major effect on the susceptibility of native starch granules to digestion by β-amylase, with waxy starch granules appearing resistant to attack, while starch granules from a high-amylose line showed significant degradation. The rate of hydrolysis of starch granules by amylases including β-amylase is also affected by granule surface area (Tester, Qi, & Karkalas, 2006; Kim, Kong, Kim, & Lee, 2008). The high amount of small granules with a proportionally larger surface area present in SW (Figs. 2B and 3B) could contribute to making intact SW starch granules less resistant to enzymatic modification.

A unique bimodal peak, representing polyglucans of lower molecular weight, was present only in SW (Figs. 5A and 6A). A debranching treatment (Fig. 5B, inset), indicated that a large portion of these polyglucans were linear malto-oligosaccharides (MOS), while the remainder represented short chains having one or two branches. The molecules in this unique peak likely arise from the activity of hydrolyzing enzymes, such as debranching enzymes, on the abnormally structured amylopectin formed in sweet wheat. The lack of amylose in combination with the less efficient synthesis of amylopectin in the double mutant may allow hydrolysis to occur prior to the crystallization process that normally protects starch granules from enzymatic degradation; such hydrolosis may be especially likely to occur in the amorphous region. Plant debranching enzymes, particularly the ISA1/ISA2 isoamylases, have the ability to debranch amylopectin (Hussain et al., 2003) to produce linear chains with a wide DP range (Takashima et al., 2007), while the branched glucans found in the bimodal peak could arise from the activity of a debranching enzyme on B-chains (chains carrying a secondary branch). Another line of evidence indicating the increased role of debranching enzyme in SW is the appearance of maltotriose in the double mutant (Fig. 4). The activity of β-amylase on a branched chain will leave a stub of either two or three

glucan units depending on the branch length, and debranching of these β-limit dextrins leads to the production of either maltose or maltotriose. It was somewhat surprising that the short molecules making up the bimodal peak were still present in starch granules that had been washed a number of times with water and SDS solution (Fig. 5), suggesting these chains were trapped within the starch granule, and were liberated only after granule solubilization. The detection of short linear molecules after the step-wise precipitation and analysis of solubilized SW starch provided further evidence of this (Fig. 7). Such chains may be involved in the formation of double helixes with other chains attached to the granule, since MOS as small as six units can form double helixes with longer molecules (Gidley & Bulpin, 1987).

Successful starch synthesis is a balancing act between the activities of starch synthases, branching enzymes, debranching enzymes, and other enzymes, and abnormal starch synthesized by mutant lines can undergo enzymatic modifications that do not normally occur during starch synthesis (Streb et al., 2008). Often, if a single starch synthase is missing, the remaining enzymes compensate to some extent, as shown by the increased level of amylose in the SSIIa null mutant and the increase in amylopectin synthesis in the Wx mutant. However, the more severe disequilibrium caused by the lack of two starch synthases may amplify the effects of relative increases in activities of other enzymes such as debranching enzymes and/or β-amylase.

SW starch lacked the A-type XRD pattern normally seen in cereals (Fig. 8), and instead processed a C-type pattern, representing a mixture of A- and B-type polymorphs, with the B-type predominating. Starch from the parental HA line also lacked a clear A-type pattern, an instead had a weakly crystalline B-type pattern dominated by V-type polymorphs. Such B- or C-type polymorphs have previously been described in high amylose cereals, including as the amylose-extender (ae) mutants of rice (Yano, Okuno, Kawakami, Satoh, & Omura, 1985) and maize (Shi et al., 1998; Yao & Janaswamy, 2011), which carry defects in starch branching enzyme IIb (SBEIIb). Interestingly, mutations in other starch synthase enzymes of cereals, such as the rice SSIIIa (Ryoo et al., 2007) or SSI enzymes (Fujita et al., 2006), did not result in a shift away from an A-type XRD pattern, further emphasizing the importance of SSIIa in amylopectin synthesis.

5. Conclusions

The absence of two important starch synthases, GBSSI and SSIIa, had dramatic and unforeseen effects on many characteristics of starch in the double mutant SW. Although SW seed appeared normal at early stages of development, starch granules were small and misshapen in appearance throughout development. The amylopectin in SW had a lower molecular weight and was less uniform than that from other genotypes, and a population of short maltooligosaccharides and small branched glucans was present only in SW starch. The changes in starch structure affected crystallinity to the degree that the normal cereal A-type diffraction pattern was lost in SW. Importantly, these results indicate that combining mutations in starch synthesis genes can result in the production of novel types of starch with structural and physiochemical characteristics that would not be predicted based on parental genotypes.

Appendix A. Supplementary data

Supplementary data associated with this article can be found, in the online version, at http://dx.doi.org/10.1016/j.carbpol.2012.04.029.

References

Balat, M., & Balat, H. (2009). Recent trends in global production and utilization of bioethanol fuel. *Applied Energy*, *86*, 2273–2282.

Blazek, J., & Copeland, L. (2010). Amylolysis of wheat starches. II. Degradation patterns of native starch granules with varying functional properties. *Journal of Cereal Science*, *52*(2), 295–302.

Buléon, A., Véronèse, G., & Putaux, J. L. (2007). Self-association and crystallization of amylose. *Australian Journal of Chemistry*, *60*(10), 706–718.

Cheetham, N. W. H., & Tao, L. (1998). Variation in crystalline type with amylose content in maize starch granules: An X-ray powder diffraction study. *Carbohydrate Polymers*, *36*(4), 277–284.

Craig, J., Lloyd, J. R., Tomlinson, K., Barber, L., Edwards, A., Wang, T. L., et al. (1998). Mutations in the gene encoding starch synthase II profoundly alter amylopectin structure in pea embryos. *The Plant Cell*, *10*(3), 413–426.

Cuevas, R. P., Daygon, V. D., Corpuz, H. M., Nora, L., Reinke, R. F., Waters, D. L. E., et al. (2010). Melting the secrets of gelatinisation temperature in rice. *Functional Plant Biology*, *37*(5), 439–447.

Demirbas, A. (2007). Progress and recent trends in biofuels. *Progress in Energy and Combustion Science*, *33*(1), 1–18.

Echt, C. S., & Schwartz, D. (1981). Evidence for the inclusion of controlling elements within the structural gene at the waxy locus in maize. *Genetics*, *99*(2), 275–284.

Ellis, R. P., Cochrane, M. P., Dale, M. F. B., Duffus, C. M., Lynn, A., Morrison, I. M., et al. (1998). Starch production and industrial use. *Journal of the Science of Food and Agriculture*, *77*(3), 289–311.

Fujita, N., Yoshida, M., Asakura, N., Ohdan, T., Miyao, A., Hirochika, H., et al. (2006). Function and characterization of starch synthase I using mutants in rice. *Plant Physiology*, *140*(3), 1070–1084.

Fujita, S., Yamamoto, H., Sugimoto, Y., Morita, N., & Yamamori, M. (1998). Thermal and crystalline properties of waxy wheat (*Triticum aestivum*) starch. *Journal of Cereal Science*, *27*(1), 1–5.

Gernat, C., Radosta, S., Damaschun, G., & Schierbaum, F. (1990). Supramolecular structure of legume starches revealed by X-ray scattering. *Starch-Stärke*, *42*(5), 175–178.

Gidley, M. J., & Bulpin, P. V. (1987). Crystallization of maltooligosaccharides as models of the crystalline forms of starch: Minimum chain-length requirement for the formation of double helices. *Carbohydrate Research*, *161*(2), 291–300.

Hayakawa, K., Tanaka, K., Nakamura, T., Endo, S., & Hoshino, T. (1997). Quality characteristics of waxy hexaploid wheat (*Triticum aestivum* L.): Properties of starch gelatinization and retrogradation. *Cereal Chemistry*, *74*(5), 576–580.

He, G. Q., Song, X. Y., Ruan, H., & Chen, F. (2006). Octenyl succinic anhydride modified early indica rice starches differing in amylose content. *Journal of Agricultural and Food Chemistry*, *54*(7), 2775–2779.

Hovenkamp-Hermelink, J. H. M., de Vries, J. N., Adamse, P., Jacobsen, E., Witholt, B., & Feenstra, W. J. (1988). Rapid estimation of the amylose/amylopectin ratio in small amounts of tuber and leaf tissue of the potato. *Potato Research*, *31*(2), 241–246.

Hussain, H., Mant, A., Seale, R., Zeeman, S., Hinchliffe, E., Edwards, A., et al. (2003). Three isoforms of isoamylase contribute different catalytic properties for the debranching of potato glucans. *The Plant Cell*, *15*(1), 133–149.

Kim, J. C., Kong, B. W., Kim, M. J., & Lee, S. H. (2008). Amylolytic hydrolysis of native starch granules affected by granule surface area. *Journal of Food Science*, *73*(9), C621–C624.

Konik-Rose, C., Thistleton, J., Chanvrier, H., Tan, I., Halley, P., Gidley, M., et al. (2007). Effects of starch synthase IIa gene dosage on grain, protein and starch in endosperm of wheat. *Theoretical and Applied Genetics*, *115*(8), 1053–1065.

Konishi, Y., Nojima, H., Okuno, K., Asaoka, M., & Fuwa, H. (1985). Characterization of starch granules from waxy, nonwaxy, and hybrid seeds of *Amaranthus hypochondriacus* L. *Agricultural and Biological Chemistry*, *49*(7), 1965–1971.

Kuroda, A., Oda, S., Miyagawa, S., & Seko, H. (1989). A method of measuring amylose content and its variation in Japanese wheat cultivars and Kanto breeding lines. *Japanese Journal of Breeding*, *39*(Suppl. 2), 142–143 (in Japanese)

Mangalika, W. H. A., Miura, H., Yamauchi, H., & Noda, T. (2003). Properties of starches from near-isogenic wheat lines with different wx protein deficiencies. *Cereal Chemistry*, *80*(6), 662–666.

Mendez-Montealvo, G., Wang, Y.-J., & Campbell, M. (2011). Thermal and rheological properties of granular waxy maize mutant starches after β-amylase modification. *Carbohydrate Polymers*, *83*(3), 1106–1111.

Morell, M. K., Samuel, M. S., & O'Shea, M. G. (1998). Analysis of starch structure using fluorophore-assisted carbohydrate electrophoresis. *Electrophoresis*, *19*(15), 2603–2611.

Morell, M. K., Kosar-Hashemi, B., Cmiel, M., Samuel, M. S., Chandler, P., Rahman, S., et al. (2003). Barley sex6 mutants lack starch synthase IIa activity and contain a starch with novel properties. *The Plant Journal*, *34*(2), 173–185.

Nakamura, T., Shimbata, T., Vrinten, P., Saito, M., Yonemaru, J., Seto, Y., et al. (2006). Sweet wheat. *Genes & Genetic Systems*, *81*(5), 361–365.

Nakamura, T., Vrinten, P., Hayakawa, K., & Ikeda, J. (1998). Characterization of a granule-bound starch synthase isoform found in the pericarp of wheat. *Plant Physiology*, *118*(2), 451–459.

Nakamura, T., Vrinten, P., Saito, M., & Konda, M. (2002). Rapid classification of partial waxy wheats using PCR-based markers. *Genome*, *45*(6), 1150–1156.

Nakamura, T., Yamamori, M., Hirano, H., & Hidaka, S. (1993). Identification of three Wx proteins in wheat (*Triticum aestivum* L.). *Biochemical Genetics*, *31*(1–2), 75–86.

Nakamura, T., Yamamori, M., Hirano, H., Hidaka, S., & Nagamine, T. (1995). Production of waxy (amylose-free) wheats. *Molecular and General Genetics*, *248*(3), 253–259.

Nakamura, Y., Francisco, P. B., Jr., Hosaka, Y., Sato, A., Sawada, T., Kubo, A., et al. (2005). Essential amino acids of starch synthase IIa differentiate amylopectin structure and starch quality between *japonica* and *indica* rice varieties. *Plant Molecular Biology*, *58*(2), 213–222.

Naqvi, S., Ramessar, K., Farré, G., Sabalza, M., Miralpeix, B., Twyman, R. M., et al. (2011). High-value products from transgenic maize. *Biotechnology Advances*, *29*(1), 40–53.

Röper, H. (2002). Renewable raw materials in Europe – Industrial utilisation of starch and sugar. *Starch-Stärke*, *54*(3–4), 89–99.

Ryoo, N., Yu, C., Park, C. S., Baik, M. Y., Park, I. M., Cho, M. H., et al. (2007). Knockout of a starch synthase gene OsSSIIIa/Flo5 causes white-core floury endosperm in rice (*Oryza sativa* L.). *Plant Cell Reports*, *26*(7), 1083–1095.

Saito, M., Vrinten, P., Ishikawa, G., Graybosch, R., & Nakamura, T. (2009). A novel codominant marker for selection of the null *Wx-B1* allele in wheat breeding programs. *Molecular Breeding*, *23*(2), 209–217.

Sarikaya, E., Higasa, T., Adachi, M., & Mikami, B. (2000). Comparison of degradation abilities of α- and β-amylases on raw starch granules. *Process Biochemistry*, *35*(7), 711–715.

Shi, Y. C., Capitani, T., Trzasko, P., & Jeffcoat, R. (1998). Molecular structure of a low-amylopectin starch and other high-amylose maize starches. *Journal of Cereal Science*, *27*(3), 289–299.

Shimbata, T., Nakamura, T., Vrinten, P., Saito, M., Yonemaru, J., Seto, Y., et al. (2005). Mutations in wheat starch synthase II genes and PCR-based selection of a SGP-1 null line. *Theoretical and Applied Genetics*, *111*(6), 1072–1079.

Shimbata, T., Inokuma, T., Sunohara, A., Vrinten, P., Saito, M., Takiya, T., et al. (2011). High levels of sugars and fructan in mature seed of sweet wheat lacking GBSSI and SSIIa enzymes. *Journal of Agricultural and Food Chemistry*, *59*(9), 4794–4800.

Singh, N., Cairns, P., Morris, V. J., & Smith, A. C. (1998). Physical properties of extruded wheat starch-additive mixtures. *Cereal Chemistry*, *75*(3), 325–330.

Stettler, M., Eicke, S., Mettler, T., Messerli, G., Hörtensteiner, S., & Zeeman, S. C. (2009). Blocking the metabolism of starch breakdown products in *Arabidopsis* leaves triggers chloroplast degradation. *Molecular Plant*, *2*(6), 1233–1246.

Streb, S., Delatte, T., Umhang, M., Eicke, S., Schorderet, M., Reinhardt, D., et al. (2008). Starch granule biosynthesis in *Arabidopsis* is abolished by removal of all debranching enzymes but restored by the subsequent removal of an endoamylase. *The Plant Cell*, *20*(12), 3448–3466.

Takashima, Y., Senoura, T., Yoshizaki, T., Haniada, S., Ito, H., & Matsui, H. (2007). Differential chain-length specificities of two isoamylase-type starch-debranching enzymes from developing seeds of kidney bean. *Bioscience, Biotechnology, and Biochemistry*, *71*(9), 2308–2312.

Tester, R. F., & Morrison, W. R. (1990). Swelling and gelatinization of cereal starches. I. Effects of amylopectin, amylose, and lipids. *Cereal Chemistry*, *67*(6), 551–557.

Tester, R. F., Qi, X., & Karkalas, J. (2006). Hydrolysis of native starches with amylases. *Animal Feed Science and Technology*, *130*(1–2), 39–54.

U.S. Department of Agriculture. (2011). *USDA agricultural projections to 2020*. OCE-111, February 2011. Washington, DC, USA.

Vandeputte, G. E., Derycke, V., Geeroms, J., & Delcour, J. A. (2003). Rice starches. II. Structural aspects provide insight into swelling and pasting properties. *Journal of Cereal Science*, *38*(1), 53–59.

Xie, F. (2011). Biodegradable starch-based nanocomposites. *Wiley Encyclopedia of Composites*.

Yamamori, M., Fujita, S., Hayakawa, K., Matsuki, J., & Yasui, T. (2000). Genetic elimination of a starch granule protein, SGP-1, of wheat generates an altered starch with apparent high amylose. *Theoretical and Applied Genetics*, *101*(1–2), 21–29.

Yano, M., Okuno, K., Kawakami, J., Satoh, H., & Omura, T. (1985). High amylose mutants of rice, *Oryza sativa* L. *Theoretical and Applied Genetics*, *69*(3), 253–257.

Yao, Y., & Janaswamy, S. (2011). Gene dosage effect on starch structure studied using maize polygenic model containing *ae* and *su1* mutant alleles. *Food Chemistry*, *125*(4), 1153–1159.

Yoo, S.-H., & Jane, J. (2002). Structural and physical characteristics of waxy and other wheat starches. *Carbohydrate Polymers*, *49*(3), 297–305.

Yu, L., Dean, K., & Li, L. (2006). Polymer blends and composites from renewable resources. *Progress in Polymer Science*, *31*(6), 576–602.

Zeeman, S. C., Kossmann, J., & Smith, A. M. (2010). Starch: Its metabolism, evolution, and biotechnological modification in plants. *Annual Review of Plant Biology*, *61*, 209–234.

Zhang, X., Colleoni, C., Ratushna, V., Sirghie-Colleoni, M., James, M. G., & Myers, A. M. (2004). Molecular characterization demonstrates that the *Zea mays gene sugary2* codes for the starch synthase isoform SSIIa. *Plant Molecular Biology*, *54*(6), 865–879.